International Journal of Research in Engineering and Science (IJRES)
ISSN (Online): 2320-9364, ISSN (Print): 2320-9356
www.ijres.org Volume 14 Issue 7 ǁ July 2026 ǁ PP. 33-40

Slope Stability Assessment and Remediation of a Landslide-Prone Road Section: A Case Study of the Paleleh–Lokodoka Road, Central Sulawesi, Indonesia

Muh. Tahir[1], Sriyati Ramadhani[2], Sukiman Nurdin[3]
[1]*Department of Civil Engineering, Tadulako University, Central Sulawesi, Indonesia*
[2,3] *Department of Civil Engineering - Geotechnical Engineering Concentration, Universitas Tadulako, Palu, Central Sulawesi, Indonesia*
Corresponding Author: sukiman@untad.ac.id

Abstract
The Paleleh-Lokodoka road section at KM 685+100 in Buol Regency, Central Sulawesi, experienced landsliding and pavement subsidence on the lower slope following intense rainfall, affecting a width of approximately 50 m with a circular slide failure pattern. This study analyzes the soil characteristics, evaluates the stability of the existing slope, and designs a slope treatment using a cantilever retaining wall (DPT) combined with bored piles. The analysis was carried out using the Finite Element Method (FEM) in Plaxis 2D with a Mohr-Coulomb soil model, in accordance with SNI 8460:2017. Field and laboratory investigations (SPT and resistivity survey) indicate a soil profile dominated by clayey sand (SM/SW) with interbedded sandy clay (CL). The existing slope analysis yielded a Factor of Safety (FS) of 0.78, far below the minimum requirement (FS >= 1.5), with a global circular failure mechanism. After installing the cantilever DPT (height 2.50 m, footing width 1.80 m) combined with bored piles (diameter 0.60 m, length 9.50 m, spacing 1.20 m), the FS increased to 1.56 under service conditions and 1.47 under seismic loading (PGA = 0.70g), with a maximum horizontal deformation of 87 mm, still within the 150 mm tolerance limit. Manual checks of the DPT against sliding and overturning under saturated conditions produced FS values of 2.84 and 1.97, respectively, both satisfying the safety requirement. It is concluded that the combination of a cantilever retaining wall and bored piles is an effective technical solution for stabilizing the slope at the study location.
Keywords: *Slope stability; retaining wall; bored pile; Finite Element Method; Plaxis 2D.*

Date of Submission: 17-06-2026 Date of Acceptance: 30-06-2026

I. INTRODUCTION

Central Sulawesi has a diverse and complex topography, making it highly susceptible to landslide hazards, particularly along national roads that traverse steep slopes. The Paleleh-Lokodoka road section at KM 685+100 in Buol Regency experienced landsliding as well as pavement and shoulder subsidence, accompanied by damage to the box culvert (deck slab), typically occurring after heavy rainfall. The landslides are localized within low-bearing-capacity embankment soil, triggered by rainwater infiltration that increases pore-water pressure and reduces the soil's shear strength. The affected area spans approximately 50 m in width, with a circular slide failure mechanism.

This condition poses a potential risk of disrupting traffic flow, increasing accident risks, and causing economic losses. Therefore, a comprehensive slope stability assessment is required to formulate an appropriate mitigation strategy. This study aims to (1) analyze the soil characteristics at the study site, (2) evaluate the stability of the existing slope, and (3) design a slope reinforcement system using a combination of a retaining wall and bored piles based on Finite Element Method (FEM) analysis using Plaxis 2D, in accordance with SNI 8460:2017.

1.1 Principles of Slope Stability and Factor of Safety

Slope stability refers to the capacity of a slope to maintain its position without undergoing failure or mass movement. Slope stability analysis is based on Limit Equilibrium and Finite Element principles, in which the Factor of Safety (FS) is calculated as the ratio of resisting forces to the driving forces causing soil movement. A slope is considered stable if FS ≥ 1.5, whereas FS < 1.5 indicates a potential for instability [4]. The shear strength of soil (τ) follows the Mohr-Coulomb failure criterion, defined as the sum of soil cohesion (c) and the product of normal stress and tan φ. An increase in pore water pressure due to rainfall infiltration reduces the effective stress and shear strength of the soil, acting as a primary driver of slope instability [5]. According to SNI 8460:2017, the minimum required FS values are 1.5 for lateral shear and global stability, 3.0 for soil bearing capacity, and 1.1 for seismic loading conditions [1].

1.2 Finite Element Method and Mohr-Coulomb Constitutive Model

The two primary methods widely used in slope stability analysis are the Limit Equilibrium Method (LEM) and the Finite Element Method (FEM). LEM assesses stability by dividing the slope into vertical slices and computing the force and moment equilibria within each slice to determine the critical FS. In contrast, FEM subdivides the soil domain into small elements (discretization), allowing for a more detailed analysis of soil deformation and stress behaviors, including the interaction between soil and structural perkuatan [8]. In this study, the soil is modeled using the Mohr-Coulomb constitutive model, which is an elasto-plastic model utilizing five primary parameters: Young's modulus (E), Poisson's ratio (ν), cohesion (c), internal friction angle (ϕ), and dilatancy angle (ψ). This model represents soil behavior using a first-order approach and is commonly implemented for preliminary geotechnical engineering analyses [8].

1.3 Mass Movement and Landslide Types

A landslide is the downslope movement of soil or rock mass under the influence of gravity, occurring when driving forces exceed the resisting forces along a slip surface [6]. Landslides can be classified into several types based on their movement mechanisms, including rockfalls, topples, translational slides, rotational slides, lateral spreads, and flows (such as debris flows and soil creep) [7]. A circular slide failure pattern commonly occurs in low-bearing-capacity embankment soils, as identified at this research site, where the soil mass moves along a curved failure surface due to soil saturation following intense rainfall events.

1.4 Retaining Walls and Bored Piles

A cantilever retaining wall is a reinforced concrete structure that relies on its self-weight and the weight of the soil above its foundation base plate to resist lateral earth pressure. The stability of a retaining wall is verified against three primary failure modes: overturning, sliding, and foundation soil bearing capacity, with minimum FS values of 1.5, 1.5, and 2.0, respectively, according to SNI 8460:2017 [1],[2]. Bored piles serve as supplemental reinforcement that resists lateral forces through shaft friction (skin friction) and end bearing resistance, with the ultimate load capacity calculated as the sum of these two components [3]. The combination of a retaining wall and bored piles is frequently used on slopes with low bearing capacity and high lateral load risks, such as landslide-prone highway embankments.

1.5 Previous Studies

Several previous studies have evaluated slope stability and mitigation designs on road sections using various methods and distinct site conditions, as summarized in Table 1. This comparison highlights the position of this study, which focuses on national road embankment failures in highly saturated clays, using a combination of a retaining wall and bored piles, analyzed numerically via FEM with Plaxis 2D, while simultaneously accounting for traffic and seismic loads.

Author (Year)	Research Focus	Method	Difference from This Study
Wicaksono & Fattah (2023)	**Toll road slope, geogrid reinforcement**	**LEM & modern reinforcement**	**Toll road location, different geometry**
Saputra & Suhendra (2022)	**Earthquake effect on cut slopes**	**LEM, rainfall effect**	**Geosynthetic reinforcement, not retaining wall/bored pile**
Rahman & Syafi'i (2024)	**Groundwater table fluctuations**	**Pseudostatic LEM**	**Cut slope, without structural combination**
Siregar & Simanjuntak (2022)	**Interlocking concrete block retaining wall**	**LEM**	**Influenced by lake water, not rainfall infiltration**
Setiawan & Nugroho (2023)	**Retaining wall**	**FEM**	**Different types of retaining structures**

Table 1. Comparison with Previous Studies

II. RESEARCH METHODOLOGY

2.1 Location and Research Framework

The study was conducted at the landslide site along the Paleleh-Lokodoka road section at KM 685+100, Buol-Gorontalo Road, West Paleleh District, Buol Regency, Central Sulawesi, at the coordinates 1.086054° N and 121.835865° E. The research framework encompasses the following stages: literature review and Plaxis software evaluation, primary and secondary data collection, soil characteristics data analysis, mathematical and FEM slope factor of safety analysis, retaining wall design and stability calculation, culminating in conclusions and recommendations.

2.2 Stratigraphy and Rock Mass Classification

2.2.1. Boring Data

Structural data for retaining walls were compiled through technical document reviews and field surveys, including working drawings, material specifications, structural dimensions, and existing conditions. Geotechnical investigation data were obtained from deep drilling at two locations (BH-01 and BH-02) to a depth of 30 m each, with Standard Penetration Tests (SPT) integrated. Laboratory testing was performed on 13 soil samples according to AASHTO, ASTM, and SNI standards, comprising sieve analysis, Atterberg limits, specific gravity, moisture content, hydrometer analysis, unconfined compressive strength (UCS), and direct shear tests.

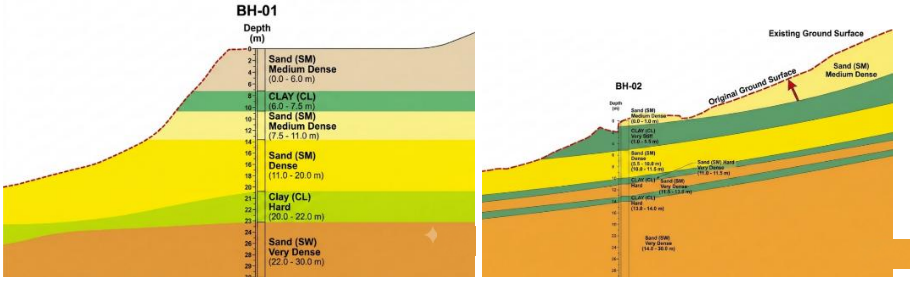

Figure 1: Stratigraphy along Cross-Section 1 through BH-01 and BH-02

2.2.2. Geoelectric Data

A 2D electrical resistivity survey using the Wenner configuration was conducted along a single survey line to identify subsurface stratigraphy and potential slip surfaces from resistivity profiles. Hydrogeological data, including monthly rainfall, were retrieved from BPS Buol Regency, indicating a peak rainfall of 413.30 mm in June. Regional geological data were obtained from the Tilamuta Geological Map Sheet, identifying the site within the Lokodidi Formation (volcanic breccia and andesite-basalt lava flows).

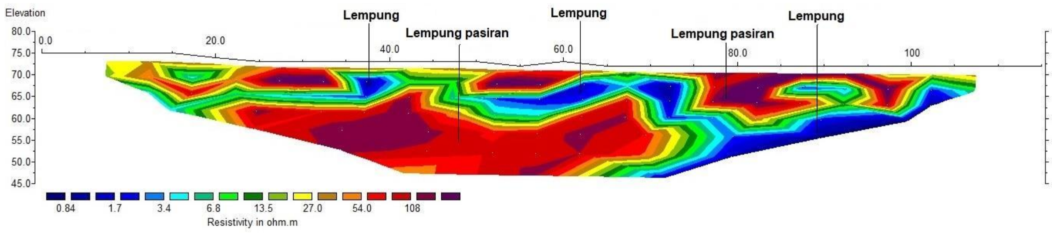

Figure 2: 2D Resistivity Distribution Section of The Survey Line

2.3 Plaxis 2D Numerical Modeling

Numerical analysis was performed using the finite element program Plaxis 2D in the following phases: general settings, geometry, material properties, initial conditions, and calculation. The slope geometry was modeled based on topographic measurements and stratigraphy derived from borehole correlations. Soil layers were modeled using the Mohr-Coulomb model, the retaining wall was defined as an elastic plate element, and the bored piles were modeled as embedded beam rows with a linear axial skin friction profile. The staged construction phases included the initial phase, construction excavation, installation of bored piles and footings, installation of the retaining wall, road backfilling and traffic loading, followed by pseudostatic analysis for seismic conditions.

2.4 Data Analysis and Stability Verification

Analysis was initially conducted on the unreinforced existing slope to establish the baseline FS. This was followed by simulating the retaining wall and bored pile reinforcement under three loading scenarios: service conditions (traffic surcharge of 15 kN/m^2 per SNI 8460:2017), pseudostatic seismic conditions ($k_h = 0.5 \times PGA$; Given a site $PGA = 0.70g$, $k_h = 0.35$), and fully saturated conditions (groundwater table rising to the embankment surface). To validate the numerical results, manual calculations of retaining wall stability against sliding, overturning, and bearing capacity failure were performed using the Coulomb/Rankine methods for lateral earth pressures and the Terzaghi, Hansen/Vesic, and other methods for soil bearing capacity, in compliance with SNI 8460:2017.

2.5 Soil Parameters for Modeling

The soil parameters input into the Plaxis 2D model were developed from laboratory test results and N-SPT correlations across the seven soil layers identified at the study site, as summarized in Table 2.

No	Soil Layers	N-SPT	γb (kN/m3)	γsat (kN/m3)	φ (deg)	c' (kN/m²)	E (kN/m²)
1	Sand SM (0-6 m)	10	14,00	16,90	29,18	8,80	$10{,}81 \times 10^3$
2	Clay CL (6-7,5 m)	14	13,50	16,90	21,95	28,04	8618
3	Sand SM (7,5-11 m)	25	13,80	17,00	31,52	11,96	$11{,}95 \times 10^3$
4	Sand SM (11-20 m)	53	14,10	16,50	32,49	12,54	$23{,}62 \times 10^3$
5	Clay CL (20-22 m)	58	13,70	16,90	21,24	21,28	$36{,}39 \times 10^3$
6	Sand SW (22-30 m)	>60	14,40	16,50	30,54	18,60	$50{,}00 \times 10^3$
7	Embankment Soil	-	15,00	16,00	30,00	5,00	$30{,}00 \times 10^3$

Table 2. Soil Layer Input Parameters

2.6 Laboratory Testing Standards

All laboratory testing procedures adhered to applicable AASHTO, ASTM, and SNI standards, as outlined in Table 3, to guarantee the consistency and precision of the soil shear strength and index properties used in the analysis.

No	Test Type	AASHTO	ASTM	SNI
1	Sieve Analysis	T-88	D-422	SNI 03-1968-1990
2	Liquid Limit (LL)	T-89-74	D-423-66	SNI 03-1967-1990
3	Plastic Limit (PL)	T-90-74	D-424-74	SNI 03-1966-1990
4	Specific Gravity of Soil	T-265	D-162	SNI 03-1964-1990
5	Moisture Content	T-265-79	D-2216	SNI 03-6989.24-2004
6	Unconfined Compressive Strength (UCS)	T-208-70	D-633-1994	SNI 03-6887-2002
7	Direct Shear	-	D-3080	SNI 03-3984-1995

Table 3. Reference Standards for Laboratory Testing

III. RESULTS AND DISCUSSION

3.1 Landslide Characteristics

Landsliding and road pavement/shoulder subsidence occurred at this location, accompanied by failure of the concrete box culvert deck slab. The movement developed on the downslope portion of the road alignment and was triggered immediately after intense rainfall events.

Figure 1: Slope Conditions Before and After Landslide

The drilling profiles from BH-01 and BH-02 demonstrate that the subsurface is predominantly clayey sand (USCS: SM/SW) interbedded with stiff-to-hard sandy clay (CL). The N-SPT values increase from medium dense ($N = 10$ to 25) at shallow depths to very dense ($N \geq 60$) at depths exceeding 22 m. Laboratory analysis yielded a cohesion range of 0.009 to 0.29 kg/cm^2 and an internal friction angle of 20° to 31° for the clayey sand layers, while the sandy clay layer exhibited higher cohesion but lower friction angles. Geoelectric resistivity data confirmed the presence of a saturated clay layer within the shallow zone, which is interpreted as the potential slip surface.

3.2 Existing Slope Stability (Unreinforced)

The stability of the unreinforced existing slope was evaluated across three scenarios in Plaxis 2D: normal conditions (static and unsaturated), pseudostatic seismic loading, and extreme fully saturated groundwater conditions.

3.2.1 Static and Unsaturated Conditions

Under the unreinforced existing baseline state, the slope was evaluated under partially saturated conditions without seismic forces. The safety phase analysis yielded a Factor of Safety (FS) of 0.78, with a maximum total displacement of 279 mm. This value falls well below the minimum threshold required by SNI 8460:2017 ($FS \geq 1.5$ for service conditions), indicating that the slope is unstable and subject to immediate global failure. Total displacement contours visualize a massive, deep circular slip surface (circular failure), with the critical strain concentration zone propagating from directly beneath the external traffic load toward the toe of the slope. An $FS = 0.78 < 1.00$ implies that the slope cannot sustain the combined self-weight of the soil and external surcharges, even in the absence of seismic acceleration or full saturation.

3.2.2 Seismic Condition Without Reinforcement

For the existing slope subjected to pseudostatic seismic loading, the horizontal seismic coefficient was determined via $k_h = 0.5 \times PGA$. Given a site PGA of 0.70g, $k_h = 0.35$, which implies that every 1,000 kN of soil mass generates a horizontal inertial force ($F_h = k_h \times W$) of 350 kN acting along the slip surface. This horizontal inertial force significantly increases the landslide driving force, further reducing the FS value below the static baseline. The unreinforced slope fails to satisfy the minimum requirement of $FS \geq 1.1$ for seismic states per SNI 8460:2017, displaying expanded displacement fields concentrated near the lower slope boundary adjacent to the roadway. This confirms that a structural reinforcement system capable of simultaneously resisting service and seismic loads is mandatory.

3.2.3 Saturated Condition Without Reinforcement

The saturated state represents the most critical scenario due to the high precipitation rates characteristic of the Buol Regency. In this simulation, the groundwater table (GWT) was modeled to rise completely to the ground surface ($h_w = H = 2.50$ m), rendering the entire soil profile fully saturated. The soil parameters utilized the saturated unit weight (γ_{sat}) from laboratory testing, and effective shear parameters (c' and ϕ') were used, since the analysis was run under drained conditions with pore-water pressures calculated independently. The active lateral earth pressure was computed based on effective stresses with $K_a = 0.392$, and the hydrostatic uplift force was determined as:

$$U = 0.5 \times \gamma_w \times h_w \times B = 0.5 \times 9.81 \times 2.50 \times 1.80 = 22.07 \text{ kN/m}$$

The elevated pore water pressure due to saturation dramatically diminishes the effective stress and soil shear strength, expanding the deformation zone across the slope mass and underscoring the necessity for a structural solution evaluated for saturation at the design phase.

FEM analysis of the unreinforced existing slope yielded a consistent baseline FS of 0.78 with a maximum total displacement of 279 mm, far exceeding acceptable structural tolerances. This falls short of SNI 8460:2017 standards ($FS \geq 1.5$), signifying a critical slope condition prone to global circular failure originating below the road alignment and extending to the toe of the slope. Under pseudostatic seismic loading, horizontal inertial forces reduce the FS further, failing the seismic safety requirement ($FS \geq 1.1$).

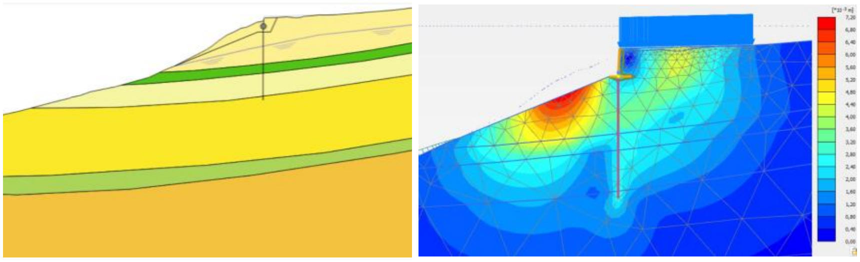

Figure 2: Geometric Modeling of the Paleleh-Lokodoka Slope KM 685+100

3.3 Mitigation Design and Performance of Retaining Wall + Bored Piles

The mitigation concept combines a cantilever concrete retaining wall with bored piles to increase global slope stability and resist lateral earth pressures. This system is optimized for slopes exhibiting unstable soil profiles, steep geometries, or substantial lateral driving forces, such as highway cut-and-fill slopes. For this project, a reinforced concrete cantilever retaining wall anchored with a bored pile row was engineered.

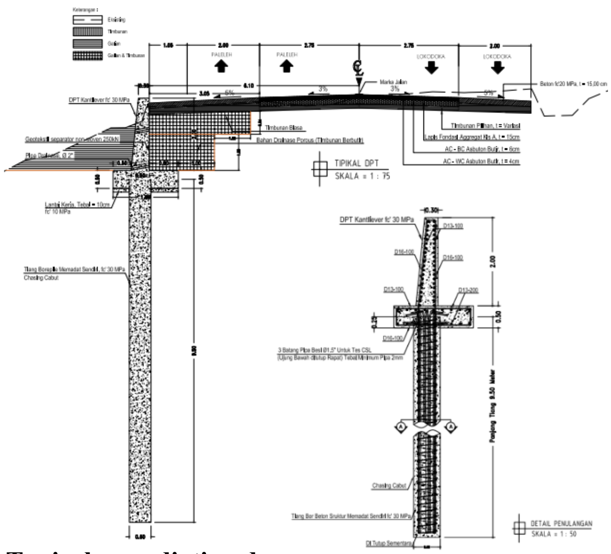

Gambar 3: Typical remediation design using retaining walls and bored piles

3.3.1 Slope Loading

The stability analysis of the slope and structural system on the Paleleh-Lokodoka road section at KM 685+100 was conducted under structural loading conditions that influence slope performance, namely, traffic surcharge (service) and seismic loads.

a. Vehicle Load (Service)
Vehicle loading was simulated as a uniform surcharge load acting on the pavement surface behind the retaining wall stem. In accordance with SNI 8460:2017 recommendations, highway traffic loading is represented as a uniform surcharge of 15 kN/m^2.

b. Seismic Load
Buol Regency and its surrounding regions are tectonically influenced by active fault systems in northern Central Sulawesi, requiring a pseudostatic slope stability validation. Based on the seismic hazard analysis, the Peak Ground Acceleration (PGA) at the research site was determined to be 0.70g.

3.3.2 Numerical Modeling Analysis Results

Finite Element Method (FEM) analysis using Plaxis 2D V23 provides a comprehensive overview of the slope behavior before and after the installation of a cantilever retaining wall combined with bored piles (diameter 0.60 m, length 9.50 m). The analysis evaluated two main operational phases: service conditions (traffic surcharge of 15 kPa) and seismic loading conditions ($PGA = 0.70g$ with $k_h = 0.35$).

The structural mitigation comprises a cantilever retaining wall (height 2.50 m, footing width 1.80 m, footing thickness 0.50 m, concrete strength $f'_c = 30$ MPa) integrated with a row of bored piles (diameter 0.60 m, length 9.50 m, spaced at 1.20 m center-to-center). The compiled FEM analysis and manual design checks are summarized in Table 1.

Condition	FS	SNI 8460:2017 Requirement	Status
Existing Slope (Unreinforced)	0,78	≥ 1,5	Unsafe
Retaining Wall + Bored Piles - Service Condition	1,56	≥ 1,5	Safe
Retaining Wall + Bored Piles - Seismic Condition	1,47	≥ 1,1	Safe
Retaining Wall - Sliding Stability (Saturated)	2,84	≥ 1,5	Safe
Retaining Wall - Overturning Stability (Saturated)	1,97	≥ 1,5	Safe

Table 1. Recapitulation of Factors of Safety (FS) for the Retaining Wall + Bored Pile System

The inclusion of the retaining wall and bored pile system raised the global slope FS from 0.78 to 1.56 under service loading and to 1.47 under seismic loading. The maximum horizontal structural deformations were limited to 3.03 mm and 87 mm, respectively, both safely below the 150 mm structural tolerance limit. Structural stability controls for the retaining wall under the critical saturated scenario—reflecting the region's high rainfall (June peak of 413.3 mm)-yielded a sliding FS of 2.84 and an overturning FS of 1.97. Furthermore, the maximum base contact stress was 89.53 kN/m^2, which is below the allowable soil bearing capacity of 130.0 kN/m^2. Thus, the proposed reinforcement system effectively manages lateral earth pressures and landslide driving forces across static, saturated, and seismic conditions.

Type of Stability Control	SF Normal Condition	SF Saturated Condition	Minimum Requirement	Status
Sliding Stability	4,87	2,84	≥ 1,5	Safe
Overturning Stability	3,33	1,97	≥ 1,5	Safe
Soil Bearing Capacity (q max)	73,47 kN/m²	89,53 kN/m²	≤ 130,0 kN/m²	Safe

Table 2. Summary of Stabilized Slope Analysis Under Saturated Conditions

3.4 Performance of the Reinforced Slope Under Specific Loading Scenarios
To complement the data in Tables 1 and 2, this section details the structural performance from the FEM analysis for each individual loading stage after slope stabilization.
3.4.1 Static and Unsaturated Conditions
The baseline analysis under standard conditions—consisting of soil self-weight and a traffic surcharge of 15 kN/m^2 without excess pore water pressures or seismic forces—yielded a global Factor of Safety (FS) of 4.87, far exceeding the minimum requirement of SNI 8460:2017 ($FS \geq 1.5$). The maximum horizontal deformation was restricted to 7.129 mm, well within the 150 mm design tolerance. Internal structural forces within the retaining wall plate element recorded a maximum bending moment of -21.37 kN·m and a maximum axial force of 82.66 kN, both falling safely within the structural capacity of the designed cross-section.
3.4.2 Seismic Condition with Reinforcement
Under seismic loading ($PGA = 0.70g$, $k_h = 0.35$The horizontal displacement increased to 87 mm due to structural reactions to the horizontal inertial forces generated by the ground acceleration. Although this deformation represents an increase compared to the service state, the reinforcement system successfully stabilized the slope mass, yielding a Safety Factor (SF) of 1.470, which complies with the SNI 8460:2017 seismic threshold ($SF \geq 1.1$). The bending moment distribution under seismic action shifted to a maximum of +9.256 kN · m and a minimum of -45.60 kN · m, demonstrating a higher structural demand relative to the static service phase (-21.37 kN · m). Axial forces concurrently increased, ranging from -76.87 kN to -116.8 kN, which dictates reinforcement detailing for the retaining wall stem and shear capacity verification for the bored piles.

3.4.3 Saturated Condition with Reinforcement
Retaining wall stability evaluations under fully saturated soil conditions accounted for a groundwater table at the backfill surface ($h_w = H = 2.50$ m), a saturated soil unit weight of $\gamma_{sat} = 16.00$ kN/m^3, an active lateral earth pressure coefficient based on effective stresses ($K_a = 0.392$), and a hydrostatic uplift pressure of:

$$U = 0.5 \times \gamma_w \times h_w \times B = 0.5 \times 9.81 \times 2.50 \times 1.80 = 22.07 \text{ kN/m}$$

The analytical results indicate that the sliding stability FS dropped from 4.87 (normal state) to 2.84 (saturated state), and the overturning stability FS decreased from 3.33 to 1.97; however, both values satisfy the minimum safety factor of 1.5 required by SNI 8460:2017. The maximum contact stress at the base increased from 73.47 kN/m^2 in the normal state to 89.53 kN/m^2 under saturation due to the added weight of water within the soil voids, remaining below the allowable bearing capacity limit of 130.0 kN/m^2. This drop in the safety factor during saturation matches the physical mechanisms of matric suction loss and elevated pore water pressures described in Section 3.2.3, underscoring that an efficient subdrainage system must accompany the structural solution.

3.5 Manual Calculations for Retaining Wall Stability
To validate the numerical finite element results, manual analytical verifications were performed on the cantilever retaining wall using Coulomb/Rankine theories for lateral earth pressures and Terzaghi/Hansen-Vesic formulations for foundation bearing capacity. The computed active (K_a) and passive (K_p) Earth pressure coefficients were 0.392 and 3.00, respectively, generating a total active lateral force of 9.88 kN/m and a total passive resisting force of 10.98 kN/m. The cumulative vertical dead load of the concrete structure and the soil block directly above the heel plate was 69.80 kN/m, yielding a total resisting moment of 55.11 kN · m.

The manual calculations showed a factor of safety against sliding (F_{gs}) of 4.87, exceeding the SNI 8460:2017 code requirement of 2.0. The factor of safety against overturning (F_{gl}) Incorporating hydrostatic uplift forces was determined to be 3.33, satisfying the minimum threshold of 1.5. The ultimate bearing capacity of the foundation soil, evaluated using Terzaghi bearing capacity factors ($N_c = 37.2$, $N_q = 22.5$, $N_\gamma = 19.7$), produced $q_u = 390.13$ kN/m^2 and an allowable bearing capacity $q_a = 130.04$ kN/m^2 using a safety factor of 3. The maximum base pressure acting on the subgrade was 73.47 kN/m^2 under normal conditions and 89.53 kN/m^2 under saturation. Both values are within the allowable bearing capacity limits, showing good agreement with the Plaxis 2D numerical simulations.

3.6 Comparison with Previous Studies

The findings of this research align with those of Siregar & Simanjuntak, who demonstrated that groundwater table elevations markedly degrade slope stability by amplifying pore-water pressure and reducing effective stress. In this study, saturation reduced the sliding FS from 4.87 to 2.84 and the overturning FS from 3.33 to 1.97, while maintaining structural safety through sizing considerations integrated during the initial design phase. Compared to the study by Setiawan & Nugroho, which utilized interlocking concrete block walls, the cantilever retaining wall coupled with a bored pile system implemented here provides superior lateral resistance via shaft skin friction and end bearing. This configuration offers better performance in low-bearing-capacity embankment zones, such as the investigated road section.

3.7 Subdrainage System and Monitoring Recommendations

Given that pore water pressure represents a critical trigger for slope degradation, an engineered drainage network is an indispensable component of the mitigation design. Recommendations include installing weep holes through the retaining wall stem spaced at 1.00 to 1.50 m intervals, lined with non-woven geotextile filters to prevent fine soil piping. Additionally, surface drainage channels along the road shoulder should be rehabilitated, and a perforated subdrain pipe network should be installed at the slope toe to accelerate post-rainfall groundwater drawdown.

A post-construction monitoring program is recommended, consisting of:

- Piezometers to record real-time groundwater fluctuations and pore water pressures.
- Inclinometers to track deep-seated lateral slope movements and structural wall deflections.
- Weekly visual inspections during the monsoon season to detect early-stage tension cracks or pavement settlement.
- An on-site manual rain gauge network to establish empirical rainfall-threshold limits for landslide warning systems at this location.

IV. CONCLUSION

The soil profile at the study site is dominated by low-bearing-capacity embankment fill and clayey sand in the shallow horizons, rendering it highly susceptible to pore-water pressure spikes from rainwater infiltration. The unreinforced existing slope is unstable, exhibiting an FS of 0.78 and a global circular failure mechanism. Slope stabilization using a concrete cantilever retaining wall with bored piles successfully increased the factor of safety to comply with SNI 8460:2017 requirements, achieving FS values of 1.56 under service states and 1.47 under seismic states, with lateral deflections remaining within allowable design limits. This structural reinforcement should be implemented alongside surface and subsurface drainage improvements to control long-term pore-water pressures, making it a viable mitigation solution for the Paleleh-Lokodoka road section at KM 685+100.

REFERENCES

[1] Badan Standardisasi Nasional. (2017). *SNI 8460:2017 Persyaratan Perancangan Geoteknik*. Jakarta: BSN.
[2] Bowles, J. E. (1996). *Foundation Analysis and Design* (5th ed.). New York: McGraw-Hill.
[3] Das, B. M. (2011). *Principles of Foundation Engineering*. Boston: Cengage Learning.
[4] Hardiyatmo, H. C. (2018). *Analisis dan Perancangan Fondasi*. Yogyakarta: Gadjah Mada University Press.
[5] Hardiyatmo, H. C. (2012). *Stabilitas Lereng Alam dan Buatan*. Yogyakarta: Gadjah Mada University Press.
[6] Varnes, D. J. (1978). *Slope Movement Types and Processes*. Transportation Research Board Special Report.
[7] USGS. (2008). *The Landslide Handbook: A Guide to Understanding Landslides*. U.S. Geological Survey.
[8] Brinkgreve, R. B. J. et al. (2024). *Plaxis 2D Material Models Manual*. Bentley Systems.
[9] Laurency, O., Andriani, Hakam, A., & Istijono, B. (2025). Penanganan Tanah Longsor pada Ruas Jalan Padang-Painan dengan Dinding Penahan Tanah dan Fondasi Tiang Bor. *Jurnal Ilmiah Rekayasa Sipil*, 22(1), 1-5.
[10] Mandagi, A. T., Ticoh, J. H., & Pudihang, E. E. P. (2024). Analisis Stabilitas dan Perkuatan Lereng dengan Metode Ground Anchor. *Tekno*, 22(88), 779-790.
[11] Setyanto, Zakaria, A., & Permana, G. W. (2016). *Analisis Stabilitas Lereng dan Penanganan Longsoran Menggunakan Metode Elemen Hingga Plaxis V.8.2*.
[12] Terzaghi, K. (1943). *Theoretical Soil Mechanics*. New York: John Wiley & Sons.
[13] USGS. (2008). *Landslide Types and Processes (Fact Sheet 2004-3072)*. U.S. Geological Survey.
[14] Cruden, D. M. (1991). A Simple Definition of a Landslide. *Bulletin of Engineering Geology and the Environment*, 43(1), 27-29.